NRIAG JOURNAL OF ASTRONOMY AND GEOPHYSICS
2022, VOL. 11, NO. 1, 21–32
https://doi.org/10.1080/20909977.2021.2005334

Phases of Magmatic Activities in South Wadi Hodein-Shalatein, Egypt: Resolving controversy about their age using Paleomagnetism and AMS

Ahmed Awad, Esmat Abd El-Aal and Ahmed Amin Khashaba

Geomagnetism Department, National Research Institute of Astronomy and Geophysics, Helwan, Egypt

ABSTRACT

Several exposures of basaltic intrusions are distributed near Red Sea coast at Wadi Hodein Southern Egypt. There is some disagreement about the palaeomagnetic pole results of these basalts; some claim it is Tertiary in age, while others claim it is of Cretaceous age. To our knowledge, no Anisotropy of Magnetic Susceptibility (AMS) results have ever been published from these rocks. Therefore, palaeomagnetic and AMS studies were performed on these basalts in order to identify phases of magmatism, paleomagnetic pole position and types of magmatic intrusions. In the present study, eight sites (219 oriented core specimens) were sampled from eight location. Rock magnetic studies reflect the presence of magnetite as the chief mineral in these rocks. Alternating field technique in association with Thermal Demagnetisation process revealed presence of one magmatic phase took place in Cretaceous age with VGP (65°N, 250°E; A_{95} = 5.3). AMS results showed that the basaltic intrusions in the study area are still holding their primary fabrics.

ARTICLE HISTORY
Received 6 April 2021
Revised 24 October 2021
Accepted 8 November 2021

KEYWORDS
Paleomagnetism; AMS; Cretaceous; Wadi Hodein; Shalatein

1. Introduction

The current study is focused on basaltic rocks that are exposed and widespread throughout the western scarps of the Red Sea coastal plain, west of Shalatin (Figure 1). The area is characterised by a Tough Mountain of the Red Sea with low to moderate isolated and conical hills and coastal plain. The studied basaltic rocks are located among latitudes (22°40′ to 23°05′ N) and longitudes (35°15′ to 35°45′ E) covering an area of about (2000 km^2) (El-Shazly 1964; El-Ramly 1972).

Previous paleomagnetic studies on the studied basalts was carried out by Niazi and Mostafa (2002). They obtained a palaeomagnetic pole position lies at 25°N, 112°E and they claim it to an Early Miocene age. Perrin and Saleh (2018) obtained a pole position that lies at 59°N, 273°E from two sites (19 samples). They stated that the pole is of a Cretaceous age.

Anisotropy of magnetic susceptibility (AMS) is a useful approach for determining the preferred orientation of magnetic minerals in a rock or unconsolidated sediments and evaluation of flow fabrics in basalts. As a result, the property is employed in the investigation of primary structures and rock fabric (Tarling and Hrouda 1993). The technique is non-destructive and can be used in nearly all types of rocks because it does not need a rock to contain specific strain markers. The method has an advantage as it can determine weak deformation even where lineation and foliation have not developed (1993).

The primary goal of studying the palaeomagnetic and magnetic fabric of this basalt is to determine its palaeomagnetic pole location and magmatism stages. The influence of the Red Sea rift's paleotectonic evolution may be determined by interpreting the acquired palaeomagnetic data and magnetic fabric.

2. Geological settings and sampling

Several authors studied the geological setting of Wadi Hodein area; Ghanem (1972); Ramadan (1994); **Egyptian Geological Survey** (EGSMA (1992) **and** EGSMA 2002); Hassan et al. (1996); Sadek et al. (1996); Sadek et al. (2000); El Amawy et al. (2000b); Hassan (2003); Sadek et al. (2003); Sadek (2004); Sadek and Hassan (2004); Obeid (2006); Sherif (2007); Abdeen et al. (2008); Hassan and Masoud (2015).

Wadi Hodein forming an alluvial fan that spreads for more than 50 km near the Red Sea coastal plain. Assemblages of recent sediments and basement rocks of Precambrian age are found and overlain unconformably by isolated hills of Cretaceous Nubian Sandstones which intruded by these basalts. The rifting of the Red Sea extrudes both rocks with NW-SE faults (Figure 2).

Basaltic rocks of south Wadi Hodein area are present as small lava flow bodies separated hills, dikes, and ridges cutting basement rocks and Nubian Sandstone of the country rocks. They are fine grained massive rocks of greenish black to black colour and

CONTACT Ahmed Awad ahmedawd4@yahoo.com EL Marsad Street 1, Helwan, Cairo, Arab Republic of Egypt, Post No: 11421 Box:138

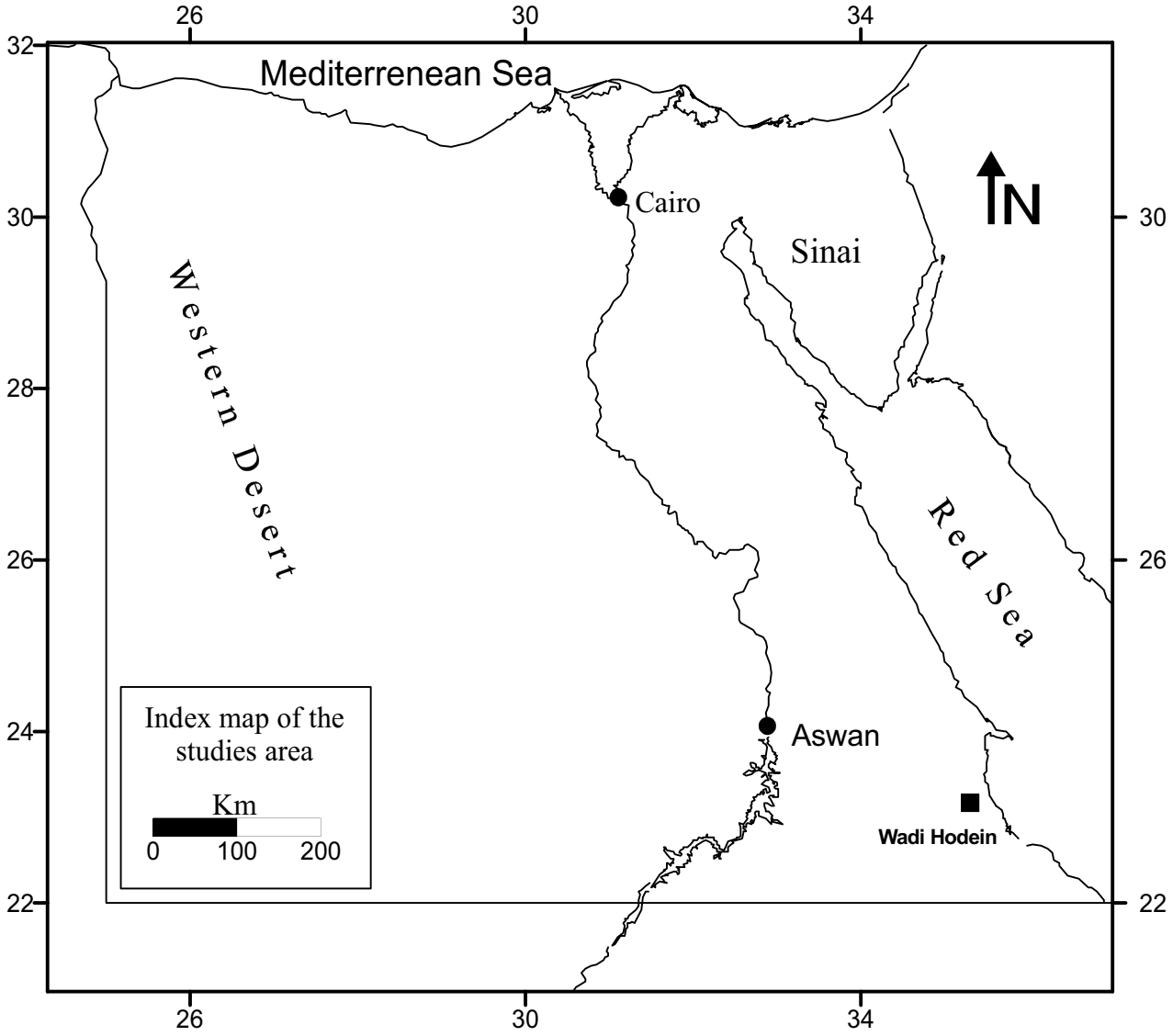

Figure 1. Map of Egypt showing the location of Wadi Hodein area.

well-developed porphyritic texture Hassan and Masoud (2015). These hills and ridges width ranging from 200 to 400 m, higher of few metres than the nearby wadis, taken NW direction that parallel to the Red Sea trending which later taken the NNW-SSE trending due to the deformation caused by the younger normal faults.

3. Rock Magnetic experiments and results

Numerous rock magnetic experiments including: Isothermal remanent magnetisation (IRM) acquisition curves, Coercivity (Back-field) curves, Hysteresis Loops (using MicroMag Magnetometer-Poland) and Curie temperature determination (using MFK-FA Kappabridge) were performed to some selected specimens of the studied rocks to distinguish the magnetic mineral(s) that may be carrying the remanent magnetisation.

During the progressive acquisition of IRM curves, the IRM intensity curve shows a fast rise up to 80–90 mT, then the saturation achieved at a field of 100–120 mT revealing of soft magnetic mineral(s) existence (Figure 3). The achieved coercivity of remanence (H_{cr}) values were ranging from 10–37 mT (Figure 4), which also refer to soft mineral(s), magnetite and/or titanomagnetite. Studies of Hysteresis loops for these specimens show similar shapes of normal Hysteresis curves with low values of coercivity (H_c) ranging from 3 to 17 mT (Figure 5). This also confirms of soft magnetic mineral(s) existence. The presence of Magnetite (soft magnetic mineral) is confirmed by its Curie temperature 570–580°C as revealed from the thermomagnetic analysis (Figure 6) of a PSD grain size (Figure 7).

Results of rock magnetic experimentations prove the presence of magnetite as the chief magnetic mineral in the studied basaltic rocks of Wadi Hodein area.

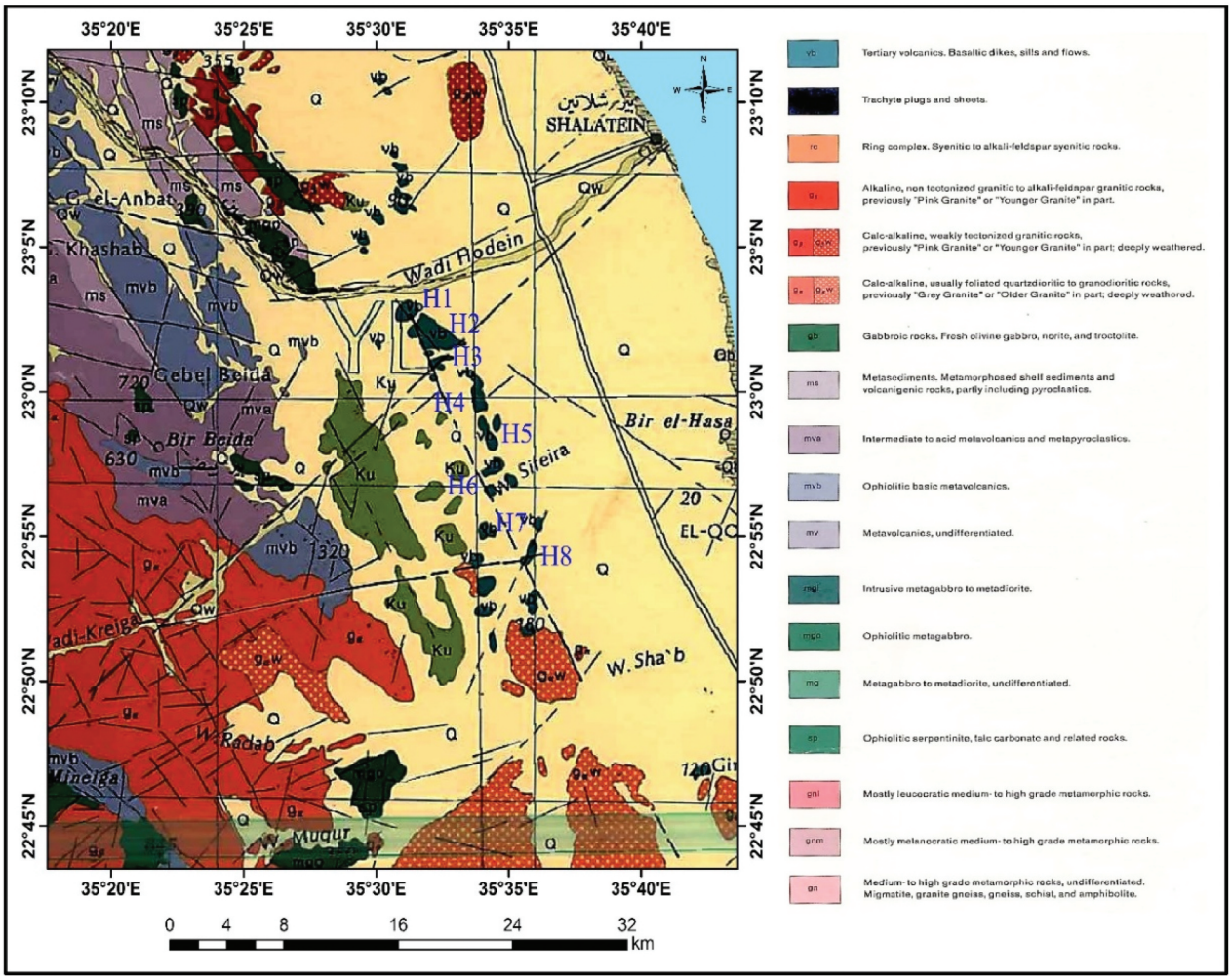

Figure 2. Geological map of Wadi Hodein area (modified after EGSMA 2002) showing the sampling location (H1–H8).

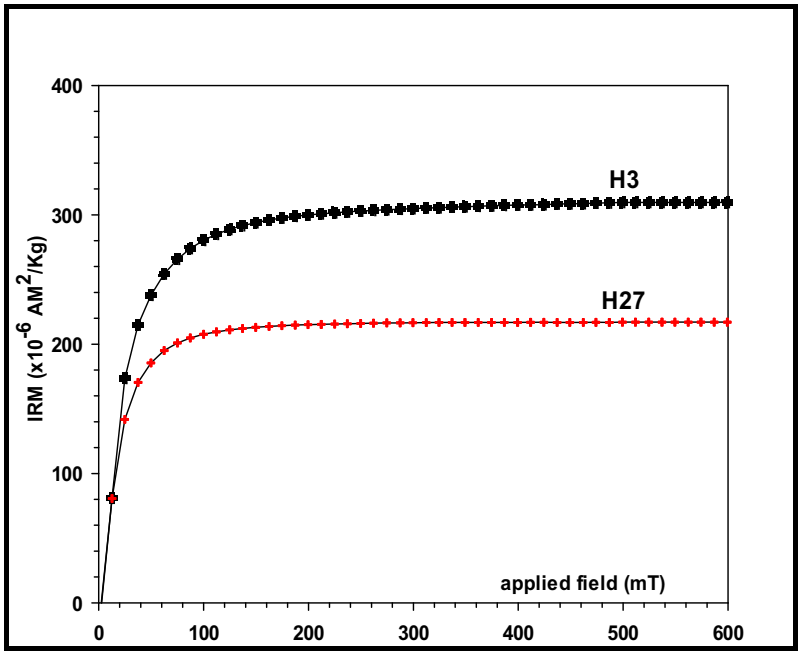

Figure 3. IRM curves for representative specimens of the studied basaltic rocks.

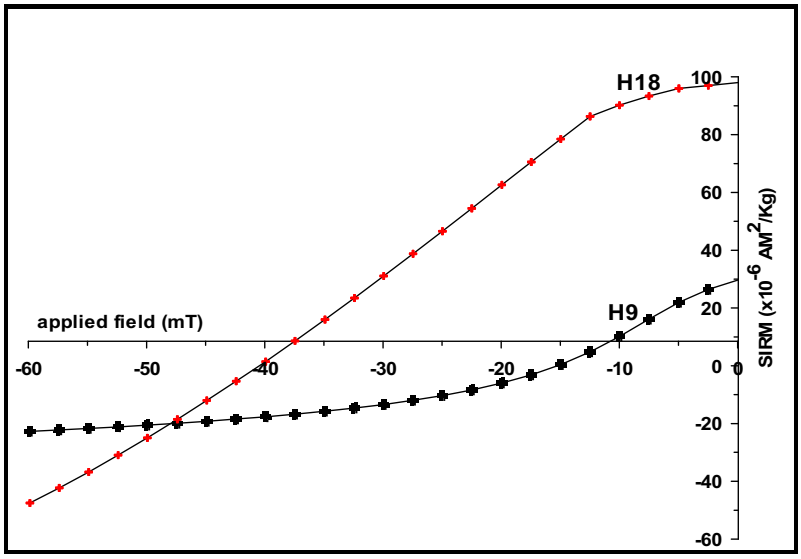

Figure 4. Coercivity curves for the studied basaltic rocks.

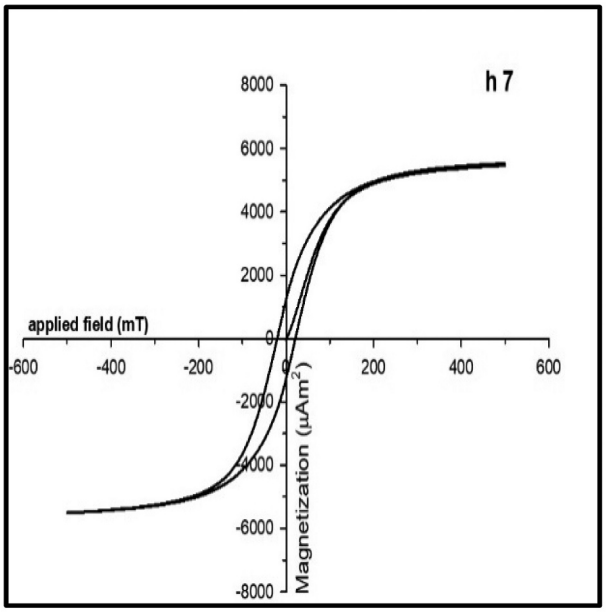

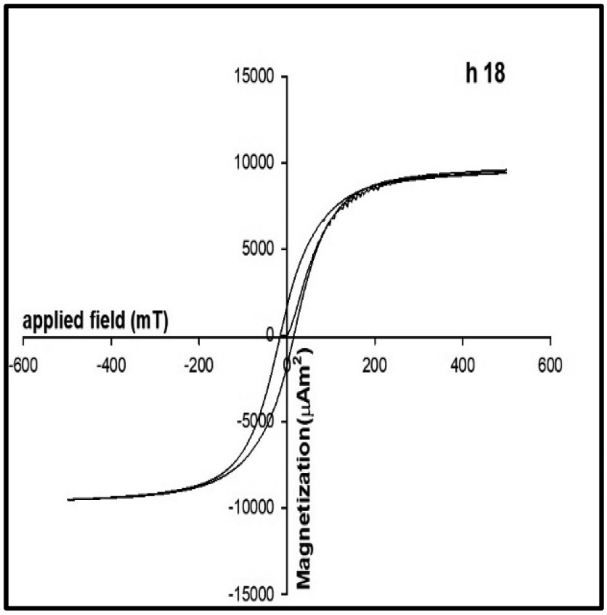

Figure 5. Hysteresis loops for typical specimens from the basalt rocks.

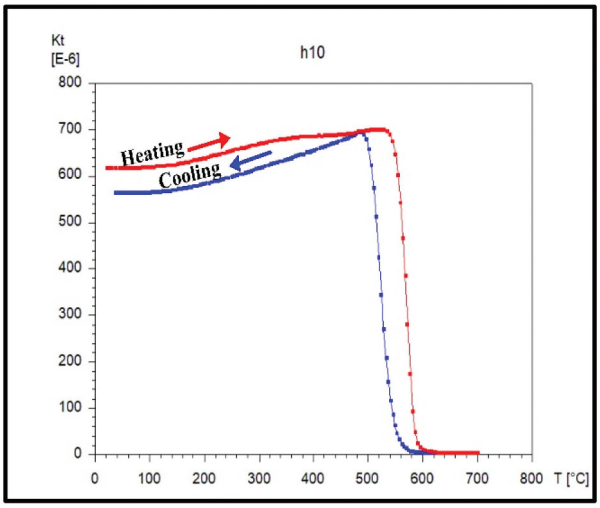

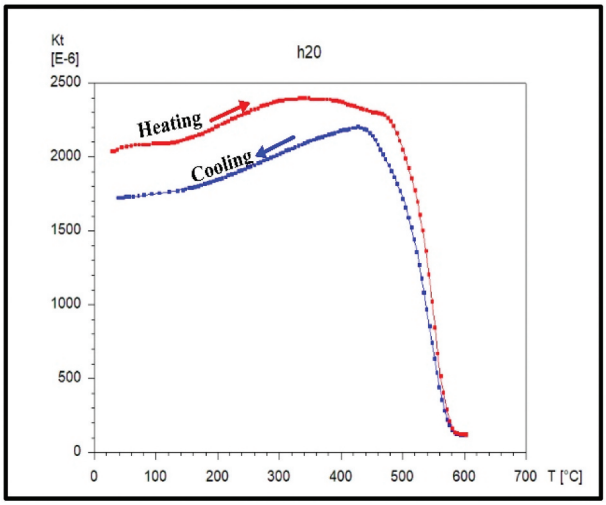

Figure 6. K-T curves showing heating/cooling sequence.

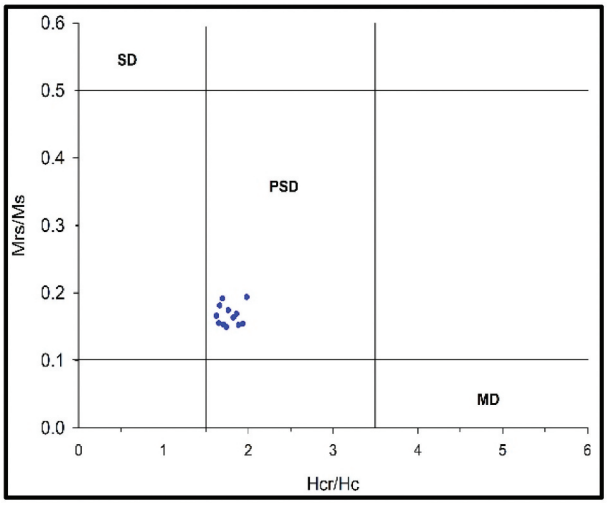

Figure 7. Day plot of some specimens from the basaltic rocks.

4. Palaeomagnetic experiments and results

Thirty-two block samples were oriented in the field and then collected from the Basaltic rocks of Wadi Hodein area. Samples were collected from a number of small, widely separate basaltic exposures covering the studied eight locations (see Figure 2). The magnetic north direction and horizontality lines were accurately drawn on each collected block sample using a magnetic compass and a balance before dislocation from the surface exposures. Using a standard fixed rock drill, a total of 219 oriented core specimens was obtained with standard dimensions of 2.2 cm height × 2.5 cm diameter. The block samples were prepared at the NRIAG Palaeomagnetism lab, while the experimental tests were carried out at both the NRIAG Palaeomagnetism lab in Helwan, Egypt, and the IGF Palaeomagnetism lab in Warsaw, Poland.

The preparation of the block samples was done at the Palaeomagnetism lab. of NRIAG, whereas the laboratory experiments have taken place in both of palaeomagnetism labs. of NRIAG, Helwan, Egypt and IGF, Warsaw, Poland.

Both types of demagnetisation analyses were executed in the present work (Alternating field (AF) and Thermal demagnetisation):

I. Alternating field (AF) demagnetisation technique was done using 2 G-SQUID (Enterprises cryogenic magnetometer with AF degausser, max. field of 160 mT) and JR6-A (automated dual speed spinner magnetometer).

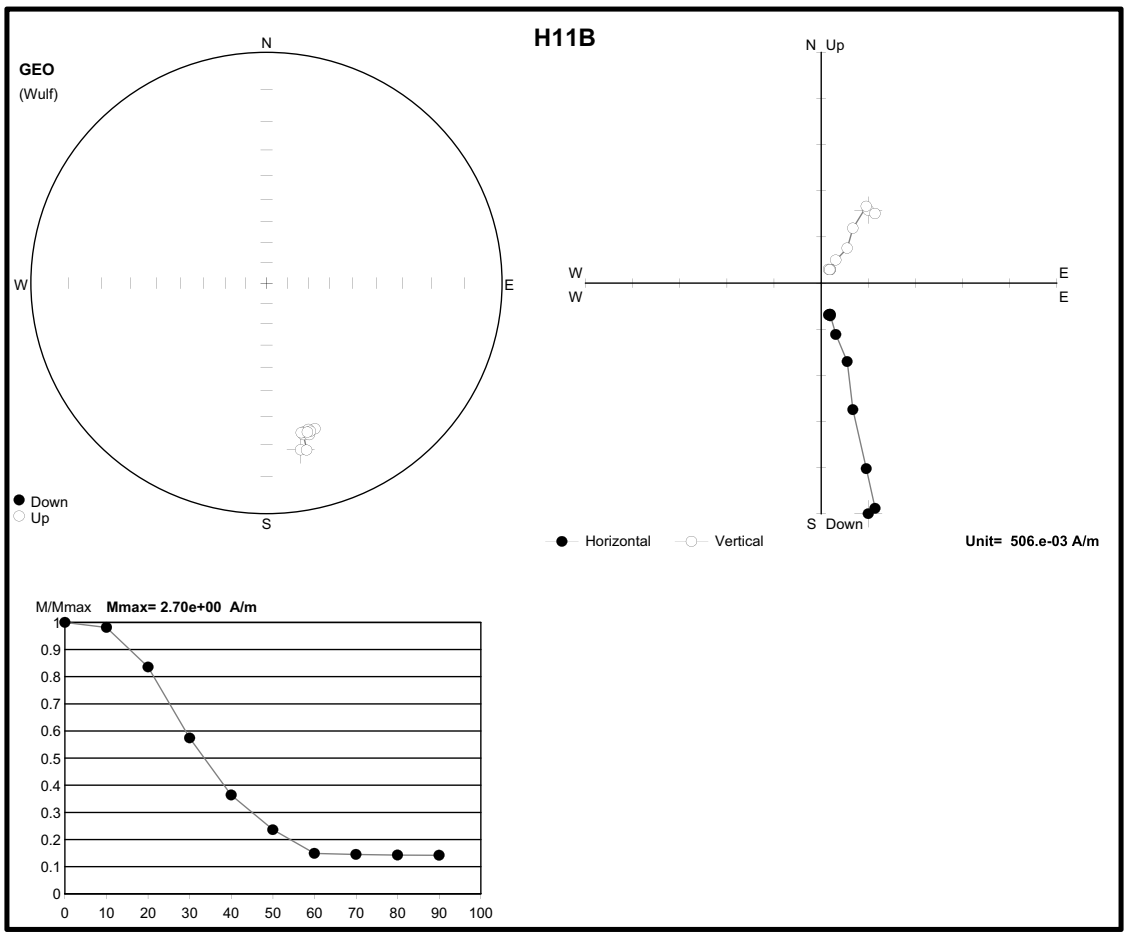

Figure 8. AF demagnetisation plots [Stereonet (north left), Zijderveld diagram (north right) (Zijderveld 1967) and intensity decay curve (down)] for a representative specimen from Wadi Hodein Basalt.

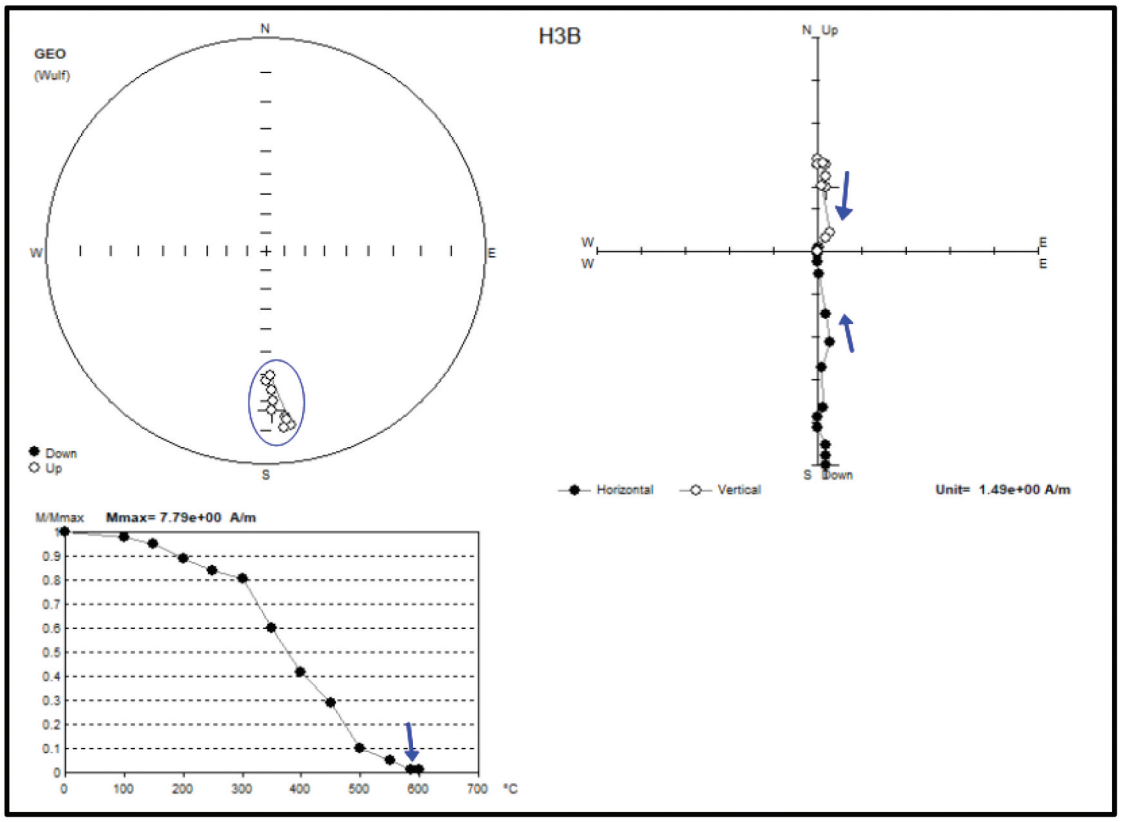

Figure 9. Plots of thermal demagnetisation for a specimen from Wadi Hodein Basalt (reverse polarity – open circle).

Table 1. Demagnetisation results of Wadi Hodein Basaltic rocks.

Site No.	*N*	*D* (°)	*I* (°)	α_{95} (°)	*K*
H1	23	83.3	−21.5	4.9	21.3
H2	30	46.2	−56.9	3.5	34.2
H3	29	49.4	−61	1.8	28
H4	25	50	−54	4	17.5
H5	27	43.6	−62.7	3.2	43.2
H6	26	32.6	−57.4	2.4	27.5
H7	30	46	−40	4.3	19.7
H8	29	32.5	−53.8	1.9	15.6
Mean	219	50.3	−52.3	12.3	21.3

In our study, initial intensities of natural remanent magnetisation (NRM) of Wadi Hodein basalt specimens are measured at first. It gives relatively high values ranging from 20 to 591 A/m, with magnetic susceptibility values (using Bartington Susceptibility Metre (MS3)) ranging from 1.16×10^{-3} to till 31.17×10^{-3} SI units. It was preferred to subject a lot of specimens to a full range AF demagnetisation to separate the characteristics remanent magnetisation from each rock specimen. Due to the presence magnetite as the chief carrier of magnetisation, the AF demagnetisation process was very efficient that gives a well and linear trajectory finalising towards the origin (Figure 8). Through the AF measurements, specimens lost their NRM intensities by increasing the demagnetising field at gradually steps of 10 mT up to a peak field of 90 mT to about of 50% from its initial value at about 30–40 mT.

II. The thermal demagnetisation was done using non-magnetic furnace (MMTD80), in which the specimens were heated gradually from 50°C up to 600°C. Examples of the thermal demagnetisation data are plotted in Figure 9.

During the thermal demagnetisation process, most of samples show gradually decrease of their remanence until it removed the great part (more than 90% of the intensity) nearly at 500–580°C.

The demagnetisation data was examined using the Remasoft 3.0 computer tool to distinguish the magnetic components. Nearly 55% of samples undergone stepwise thermal demagnetisation, and about 45% demagnetised using stepwise alternating field (AF). Both tools yielded the same ChRM directions (Figures 8 and 9). Most basaltic specimens give a high-temperature component ~580 °C with relatively high-coercivity ~60 mT.

Palaeomagnetic directions are determined using principal component analysis (Table 1 and Figure 10). Finally, eight palaeomagnetic locations yield an overall-mean direction of D = 50.3°, I = −52.3°, α_{95} = 5.3° (Figure 11). The mean of the corresponding Virtual Geomagnetic Poles (VGPs) was then determined using the Fisher statistics (Fisher 1953) representing the palaeomagnetic pole position for studied Wadi Hodein Basalts (Table 2 and Figure 12).

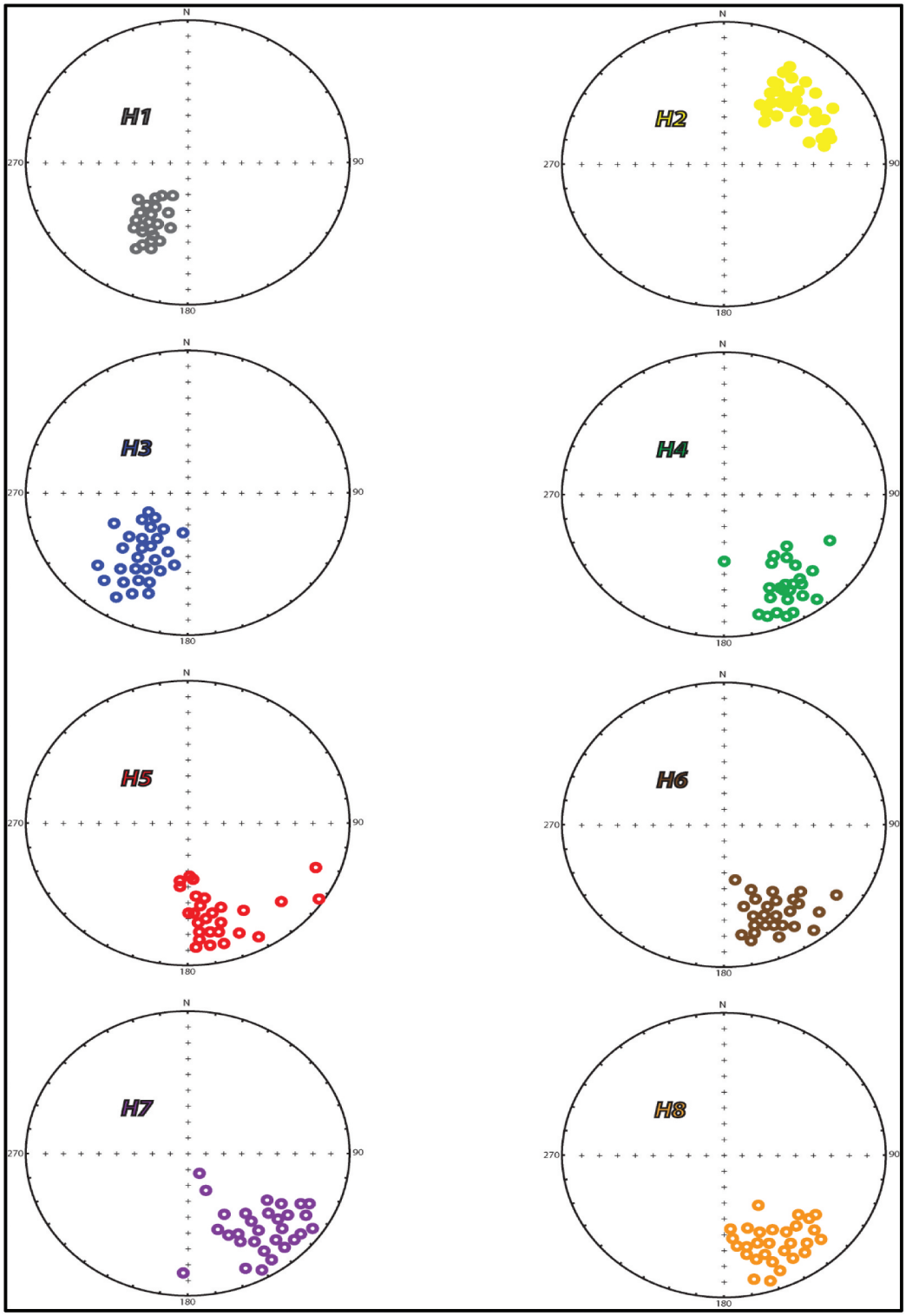

Figure 10. Equal area projection for components from eight studied locations.

where; *N*: Specimen numbers, *D*: Declination, *I*: Inclination, α_{95}: Radius of 95% circle of confidence for mean direction, *K*: Precision parameter (Fisher 1953).

5. Magnetic fabric

AMS determinations were done for a total of 99 specimens covered only six locations from the studied basaltic rocks in Wadi Hodein area. Using of a MFK1-FA Kappabridge susceptibility metre at Palaeomagnetism Lab. of IGF at Warsaw-Poland; the Low-field anisotropy of magnetic susceptibility (AMS) for all specimens were measured. The magnitudes of the principal axes of the AMS ellipsoid, which denoted (K_{max} = magnetic lineation, intermediate K_{int} and K_{min} = magnetic foliation) were determined for all specimens following by a sequence of 15 susceptibility measurements along

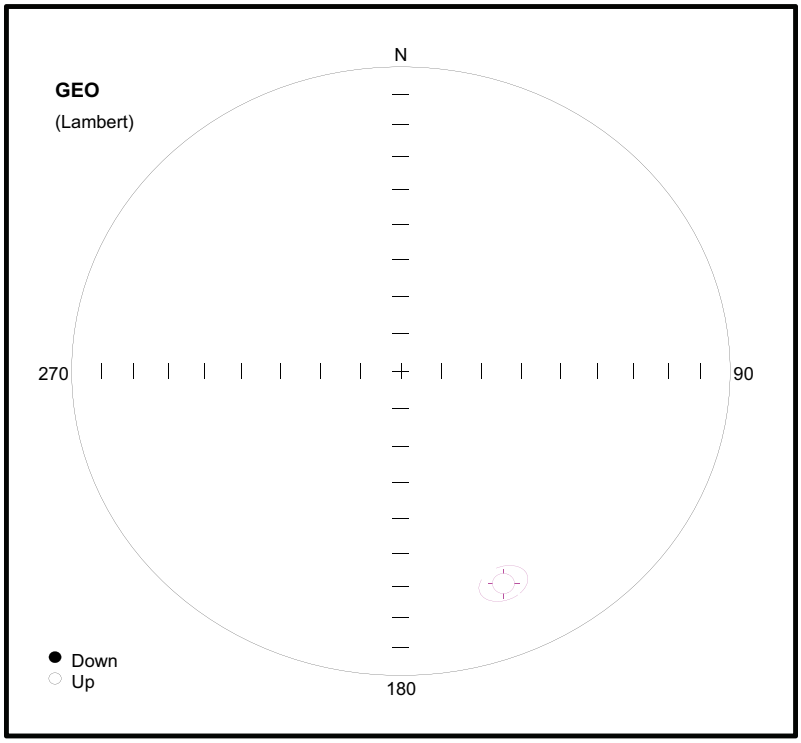

Figure 11. Mean direction for eight locations.

Table 2. Present palaeomagnetic pole and selected previous Poles from Egypt.

			Paleopole			
Reference	Location	Age (MA)	P_lat	P_long	*K*	A_{95}
1 – Hussien & Aziz (1983)	Owienat	82	77	258	34	9
2–Abd El-All (2004)	Naga	140	68	268	26	5
3 – Lotfy (2011)	Natash	82	67	229	42	5
4 – El-Shayeb et al. (2013)	Six Hills	145	78	294	22	8
5 – Mostafa et al. (2016)	Qatrani	83	78	280	25	5
6 – Present Study	Wadi Hodein		65	250	59	5.3

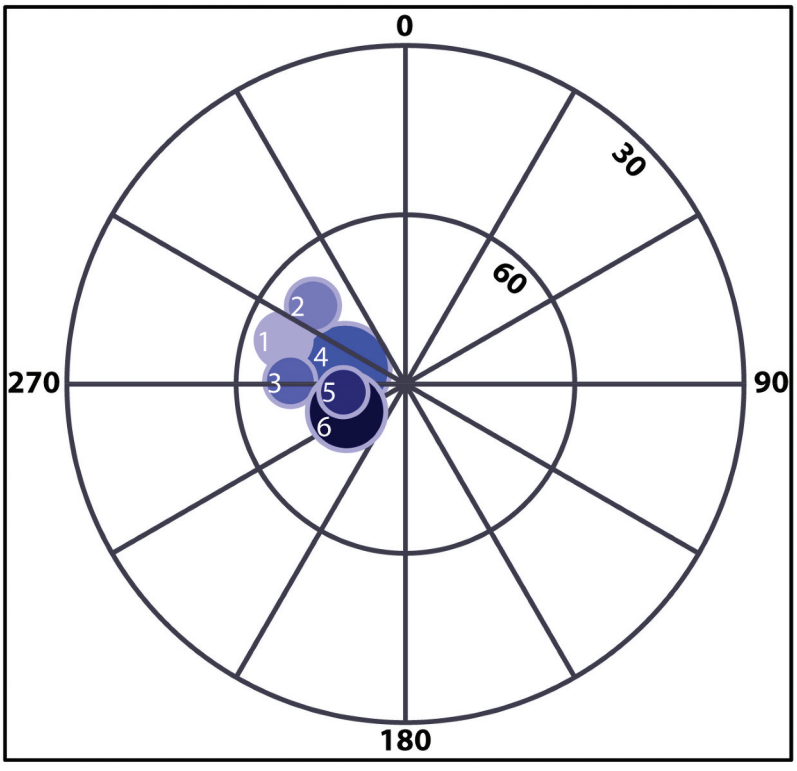

Figure 12. Present palaeomagnetic pole and selected previous Poles.

Table 3. AMS parameters for six locations with its site-mean magnetic susceptibility (*K*).

Location	N	K_m (10^{-2} SI)	P′	T	L	F	K_{max} (D/I)	K_{int} (D/I)	K_{min} (D/I)
H1	16	1.41	1.030	0.187	1.013	1.016	171/42	322/45	67/15
H2	22	4.35	1.023	0.103	1.010	1.013	29/7	283/66	122/23
H3	13	5.35	1.017	0.625	1.003	1.013	65/23	325/23	195/56
H4	13	11.2	1.016	0.361	1.004	1.011	259/9	168/2	67/80
H5	18	8.65	1.025	0.179	1.009	1.015	76/25	342/9	234/64
H6	17	0.782	1.024	0.188	1.010	1.013	274/71	184/0.3	93/19
Summation	99	– – -	– –	– –	– –	– –	– – –	– – – -	– – –
Mean	– -	5.04	1.004	0.213	1.002	1.003	– -	– -	– -

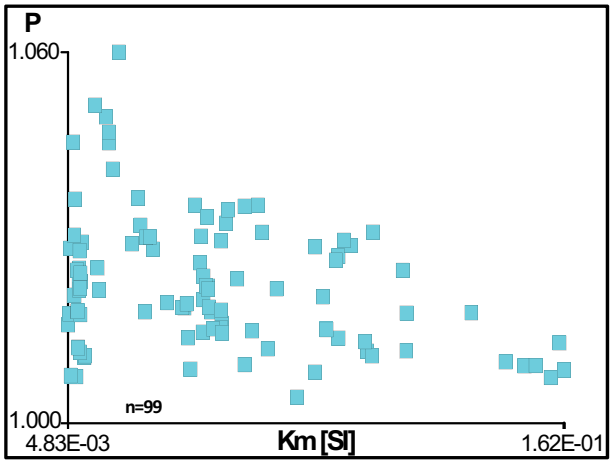

Figure 13. P/K_m curve for the studied basaltic rocks.

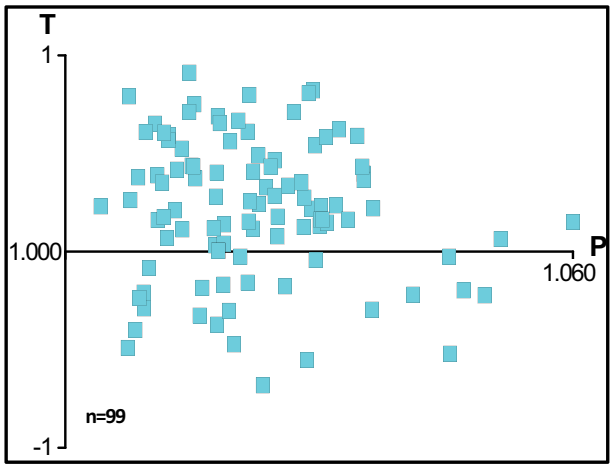

Figure 14. *T/P* curve for the studied basaltic rocks.

different orientations (Jelinek 1981). AMS for magnetite grains is controlled by the shape-preferred orientation of the individual grains (Rochette et al. 1992). The results were then examined using *Anisoft-5* software package.

The AMS parameters and mean magnetic susceptibility (K_m) after (Jelinek 1981; Tarling and Hrouda 1993) of our studied specimens are presented in (Table 3). The overall susceptibility values fall in the range of $4.83 \times 10^{-3} < K$ (SI)$< 1.62 \times 10^{-1}$ (Table 3 and Figure 13). This variable magnitude reflects the contribution of ferromagnetic grains to AMS results. In spite of the high value of susceptibilities, the anisotropy degree (*P'*), which is indicative to the degree of deformation is relatively low. It is usually less than 10% in most basaltic lava flows, dykes and sills (Tauxe 1998). Values of magnetic lineation *L* and magnetic foliation *F* are rather weak with overall site-mean (T- ellipsoid shape) value of 0.213, in the range of $0 < T \leq 1$, confirming the predominance of foliation over lineation (strong oblateness planar fabric) (Figure 14).

Where, N: specimen numbers, $\boldsymbol{K_m} = (K_1 + K_2 + K_3)/3$,

$\boldsymbol{P'} = exp\sqrt{\{2[(\eta_1-\eta_m)^2 + (\eta_2-\eta_m)^2 + (\eta_3-\eta_m)^2}$,

Where: $\eta_1 = ln\ K_1$, $\eta_2 = ln\ K_2$, $\eta_3 = ln\ K_3$ and $\eta_m = \sqrt[3]{\eta_1.\eta_2.\ \eta_3}$

$\boldsymbol{T}$: $= [2\ ln\ (K_2/K_3)/ln\ (K_1/K_3)] - 1$, $\boldsymbol{L} = K_1/K_2$, $\boldsymbol{F} = K_2/K_3$.

Despite the weak magnetic anisotropy of the volcanic rocks, measurements of AMS reflects relations between magnetic fabric and flow direction; in which the K_{max} axis tend to be parallel to the flow direction and K_{min} axis tend to be perpendicular to the flow plane (Canon-Tapia 2004). The AMS ($K_{max} \geq K_{int} \geq K_{min}$) eigenvectors in all stereograms are well grouped with narrow confidence ellipsoid, so the mean of principal susceptibility axes is statistically significant (Figure 15). Although the anisotropy is low, the magnetic foliations with slight girdle are consistent between the sites. Together with NE-SW trending (K1) magnetic lineation, may suggest some weak secondary tectonic (deformational NW-SE component) to AMS.

Analysis of the resulted AMS data (Table 3 and Figure 15) show that; sites (H1, H2 and H6) exhibit oblateness planar fabrics. H1 has less well-defined susceptibility fabric, while H2 fabric is typically planar of sub-horizontal lineation with NE trending foliation. Although the degree of anisotropy is low for sites (H3, H4) with predominance of foliation over lineation, it shows strong oblateness fabrics and exhibits planar and weakly linear ellipsoid. Site H4 has a vertical fabric that subject to low degree of deformation after lava flow and H3 and H6 exhibit an inverse magnetic fabric.

n = number of specimens.

n = number of specimens.

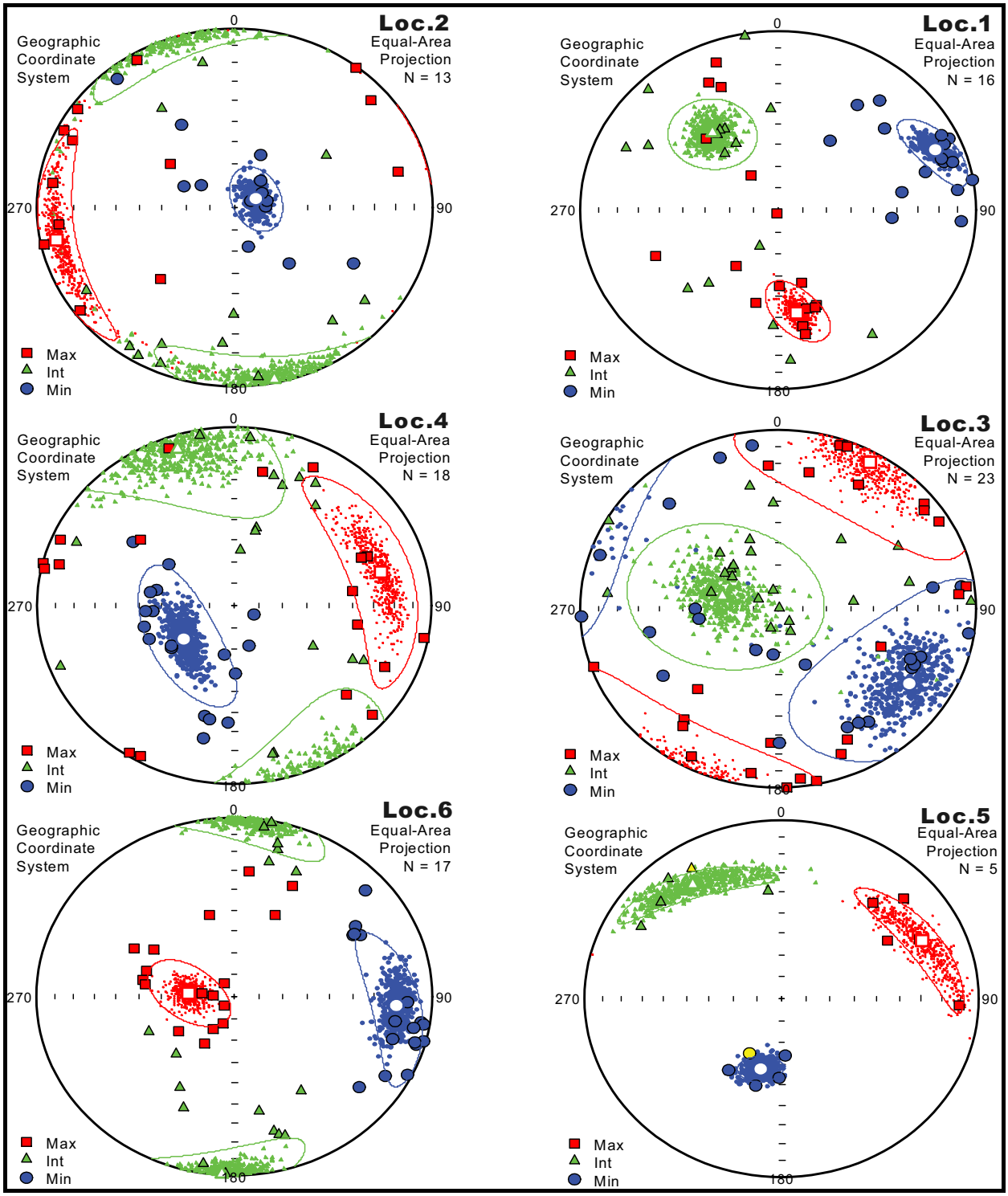

Figure 15. Equal-area projection of the in-situ directions of magnetic susceptibility principal axes.

6. Discussion

Thorough palaeomagnetic investigation done to basalts of Wadi Hodein South Eastern Egypt along Red Sea coast. 8 locations, 35 sites and 219 samples were exposed to numerous rock magnetic experiments (IRM, Back Field, Hysteresis loop and Susceptibility against Temperature), demagnetisation (Thermal and AF) and AMS measurements. Magnetite have been found to be the main magnetic mineral. Weak secondary components that may have been originated isothermally were found during data analysis and easily cleaned during demagnetisation. Primary palaeomagnetic component have been obtained from all sites, and a new pole of Cretaceous age proposed and compared with 5 previous published poles for Mesozoic in Egypt (Table 2 and Figure 12).

Magnetic Susceptibility and their anisotropy of Basaltic intrusion of Wadi Hodein area show a weakly developed fabric with low degree of an isotropy that is most probably reflects of primary

magnetic origin of different types (dykes and flows), that is further affect with the minor faults of NW orientation.

Disclosure statement

No potential conflict of interest was reported by the author(s).

ORCID

Ahmed Awad http://orcid.org/0000-0001-6680-9142
Ahmed Amin Khashaba http://orcid.org/0000-0001-6359-0464

References

Abd El-All EM. 2004. Paleomagnetism and rock magnetism of El-Naga ring complex South Eastern Desert, Egypt. NRIAG J Geophysics 3(1):1–25.

Abdeen MM, Sadek MF, Greiling RO. 2008. Thrusting and multiple folding in the Neoproterozoic basement of Wadi Hodein area, south Eastern Desert of Egypt. Accepted manuscript, J African Earth Sci (In Press. 52(1–2):21–29. doi:10.1016/j.jafrearsci.2008.03.003.

Canon-Tapia E. 2004. Anisotropy of magnetic susceptibility of lava flow and dykes: a historical account. Geol Soc, Lond, Spec Publ 238(1):205–225. doi:10.1144/GSL.SP.2004.238.01.14.

EGSMA. 1992. Baranis quadrangle map, scale, 1:250,000. Egypt (Cairo):Geol. Survey.

EGSMA. 2002. Geologic map of Marsa Shaab quadrangle, Egypt, scale, 1:250,000. Egypt (Cairo):Geol. Survey.

El Amawy MA, Wetait MA, El Alfy ZS, Shweel AS. 2000b. Geology, geochemistry and structural evolution of Wadi Beida area, south Eastern Desert, Egypt. Egypt J Geol. 44 (1):65–84.

El-Ramly MF. 1972. A new geological map for the basement rocks in the eastern and south-western Egypt. Ann Geol Survey Egypt II. 1–17.

El-Shayeb H, El-Hemaly IA, Abdel Aal E, Saleh A, Khashaba A, Odah H, Mostafa R. 2013. Magnetization of three Nubia Sandstone formations from Central Western Desert of Egypt. NRIAG J Astron Geophysics. 2(1):77–87. doi:10.1016/j.nrjag.2013.06.011.

El-Shazly EM. 1964. On the classification of the Precambrian and other rocks of magmatic affiliation in Egypt. Proc 22nd Intl Geol Congr. 10: 88–101. New Delhi.

Fisher RA. 1953. Dispersion on a sphere. Proc: R Soc London Ser 217:295–305.

Ghanem M. 1972. Geology of Wadi Hodein area. Ann Geol Survey Egypt. 2:199–214.

Hassan AS, Masoud SM. 2015. Geology and geochemistry of Tertiary basalt in south Wadi Hodein area, South Eastern Desert, Egypt. Arabian J Geo. doi:10.1007/s12517-012-0525-6

Hassan MM, Abu El Leil I, Shalaby IM, Ramadan TM. 1996. Geochemical studies on silver-gold mineralization at Wadi Hodein area, south Eastern Desert, Egypt. Proc Geol Survey Egypt Cent Conf 369–389.

Hassan SM (2003): Geo environmental study in Shalatein area, South Eastern Desert of Egypt using remote sensing and GIS techniques. MSc. Thesis. Institute of Environmental Studies and Research, Ain Shams University, Cairo (Egypt).

Hussain and Aziz (1983). Paleomagnetism of Mesozoic and Tertiary rocks from East El Owienat area south Egypt J. Geophysics. Res., 88 (1983), pp. 3523–3529.

Jelinek V. 1981. Characterization of the magnetic fabric of rock. Tectonophysics. 79(3–4):63–67. doi:10.1016/0040-1951(81)90110-4.

Lotfy HI. 2011. Active concomitant counterclockwise rotation and northwards translation of Africa during the Albian–Campanian time: a paleomagnetic study on the Wadi Natash alkaline volcanic province (104–78Ma), South Eastern Desert, Egypt. Palaeogeography, Palaeoclimatology, Palaeoecology. 310(3–4):176–190. doi:10.1016/j.palaeo.2011.07.005.

Mostafa R, Khashaba A, El-Hemaly IA, Takla EM, Abdel Aal E, Odah H. 2016. 1st paleomagnetic investigation of Nubia Sandstone at Kalabsha, south Western Desert of Egypt. NRIAG J Geo 5(1):254–262. doi:10.1016/j.nrjag.2015.12.002.

Niazi H, Mostafa MO. 2002. A paleomagnetic study of the Tertiary basaltic lava flows around Wadi Hodein Shalatein area, south Eastern Desert, Egypt. Annals Geol Survey, Egypt. XXV:429–442.

Obeid MA. 2006. The Pan-African arc-related volcanism of the Wadi Hodein area, south eastern Desert, Egypt. Petrological and geochemical constraints. J African Earth Sci. 44(3):383–395. doi:10.1016/j.jafrearsci.2005.12.007.

Perrin M, Saleh A. 2018. Cenozoic to cretaceous paleomagnetic dataset from Egypt: new data, review and global analysis. Earth Planet Sci Lett. 488:92–101. doi:10.1016/j.epsl.2018.02.014.

Ramadan TM (1994): Geological and geochemical studies on some basement rocks at Wadi Hodein area, South Eastern Desert, Egypt. Ph. D. Thesis, Faculty of Science, Al Azhar University, Cairo, 188 p.

Rochette P, Jackson M, Aubourg C. 1992. Rock magnetism and the interpretation of anisotropy of magnetic susceptibility. Rev Geophysics 30(3):209–226. doi:10.1029/92RG00733.

Sadek MF. 2004. Discrimination of basement rocks and alteration zones in Shalatein area, Southeastern Egypt using Landsat TM Imagery data. Egypt. J Remote Sens Space Sci. 7:89–98.

Sadek MF, El-Malky MG, Yehia MA, Hassan SM. 2003. Remote sensing signatures of some rock units in Shalatein area, South Eastern Desert of Egypt. J Environ Sci, Inst Environ Sci Ain Shams Univ 7 (2):407–428.

Sadek MF, Hassan SM (2004): Geo-environmental studies in Shalatein area, south Eastern Desert, Egypt using remote sensing and GIS techniques. In: 8th Int. Conf. Jord. Geol. Assoc., Amman, Jordan (Abstract).

Sadek MF, Masoud MS, Abdel Mola AF, EL-Sherbeni HA, Makhlouf AA, Hamouda EM, Mousa MA, EL-Sherif AS. 2000. Geology of Wadi Hawdayn area, South Eastern Desert, Egypt. Internal report. Geol Survey Egypt, pp. 201-221.

Sadek MF, Tolba MI, Youssef MM, Abdel Gawad GM, Salem SM, Atia SA. 1996. Geology of Wadi Kreiga-Gabal Korbiai area, South Eastern Desert, Egypt. Egypt (Cairo): Internal Report, Geol. Survey.

Sherif H.M. 2007. Petrography, geochemistry and K–Ar ages of Paleogene basalts, west Shalatein, south Eastern Desert. The Fifth International Conference on the Geology of Africa, 23–24 October 2007 Assiut-Egypt.

Tarling DH, Hrouda F. 1993. The magnetic anisotropy of rocks. London: Chapman and Hall; p. 217.

Tauxe L. 1998. Paleomagnetic principles and practice: modern approach in geophysics. Amsterdam: Kluwer Acad.

Zijderveld J. 1967. A.C. demagnetization of rocks-analysis of results. In: Colllinson DW, Creer KM, RuncornSK, editors. Methods in rock magnetism and paleomagnetism. Amsterdam (The Netherlands): Elsevier; p.254–286.